COMPARING PP AND PS SEISMIC CHARACTERIZATION OF FRACTURES IN THE MISSISSIPPIAN MERAMEC AND OSAGE INTERVALS OF THE STACK PLAY, OKLAHOMA

By

MICHAEL DAKOTA MULLEN
Bachelor of Science in Geology
Oklahoma State University
Stillwater, Oklahoma
2019

Submitted to the Faculty of the
Graduate College of the
Oklahoma State University
in partial fulfillment of
the requirements for
the Degree of
MASTER OF SCIENCE
May, 2022

COMPARING PP AND PS SEISMIC

CHARACTERIZATION OF FRACTURES IN THE

MISSISSIPPIAN MERAMEC AND OSAGE

INTERVALS OF THE STACK PLAY, OKLAHOMA

Thesis Approved:

Dr. Ahmed Ismail

Thesis Adviser

Dr. James Puckette

Dr. Mohammed Ibrahim

ACKNOWLEDGEMENTS

Most importantly I would like to thank my wife Carli for her constant support during my time in graduate school. We have been through a lot during this time and you have always been by my side. The work put into this thesis would not have been possible without your constant love and determination and for that I will always be thankful.

I would like to convey my deepest gratitude to my advisor Dr. Ahmed Ismail for his constant support and guidance throughout my time here. You are a great inspiration to all of your students and always have their best interest in mind.

I would also like to thank my committee members Dr. Jim Puckette and Dr. Mohammed Ibrahim for their advice and inspiration. Without the support and advisement from all my committee members this thesis would not have been possible. I am very thankful for this chance to work on this particular topic for my master's thesis, for which I learned so much from.

I thank Devon Energy Corporation for supplying the data used in this research. I would also like to thank CGG for the donation of the software used to complete this project.

I would also like to thank everyone in the Geophysics Research lab, Oluseun Sanuade, Zonaed Sazal, Salman Abbasi, and Patrick Meese for their constant support throughout my master's thesis, as well as their friendship during my time at Oklahoma State University.

Name: MICHAEL DAKOTA MULLEN

Date of Degree: MAY, 2022

Title of Study: COMPARING PP AND PS SEISMIC CHARACTERIZATION OF FRACTURES IN THE MISSISSIPPIAN MERAMEC AND OSAGE INTERVALS OF THE STACK PLAY, OKLAHOMA

Major Field: GEOLOGY

Abstract:

Fractures often provide a mode of secondary porosity and significantly improve rock permeability and reservoir quality. This study characterized fractures within the Mississippian Meramec and Osage intervals of the STACK play in central Oklahoma using the converted mode PS seismic data (waves propagate down as P-wave and reflect as S-wave). The study also evaluated the efficacy of the PS data for fracture characterization by comparing the results of this study with a previous seismic PP (waves propagate down as P-wave and reflect as P-wave) study of the same geological intervals and the shear wave dipole-dipole sonic log. The study adopts a seismic-based fracture characterization workflow that integrates multiple seismic attributes and builds a Discrete Fracture Network (DFN) to better describe fractures density and orientation. The PS data showed the highest concentration of fractures in the westernmost area of the PS survey with a strike direction ranging from ~90-150 degrees, which correlates well with the fractures in the shear wave dipole-dipole sonic log. Comparing the DFN from the PP and PS seismic data indicates a good correlation between the results of the two seismic data sets. However, the PP data showed slightly more fractures, likely due to the higher frequency of the PP data, with a slightly different orientation from the fractures from the PS data. The shear wave dipole-dipole sonic log showed fractures with orientations that correlate with both the PP and PS fractures. Based on the results of this study, PP and PS data showed similar large-scale fractures; however, PS data have resolved fractures that were not characterized by the PP data. The study confirms the need to include joint PP-PS fracture characterization for a more robust fracture characterization of a reservoir. Joint interpretation of the PP and PS seismic data is highly recommended for better fracture characterization of a given reservoir instead of relying only on the analysis of PP seismic data.

TABLE OF CONTENTS

LIST OF EQUATIONS

LIST OF FIGURES

Table Page

CHAPTER I

INTRODUCTION

Understanding the complex geometry of fractured carbonate reservoirs requires integrating multiple data types. Conventional PP (down and up travelling primary waves) seismic reflection methods have dominated the oil and gas exploration for decades. However, advancements in technology lead to better understanding of differing seismic waves, which have been used by researchers to better understand the subsurface (Stewart et al., 2002; Stewart et al., 2003). Recently, converted-mode or PS (waves propagate down as P-wave and reflect as S-wave) seismic data is often acquired during the acquisition phase within the oil and gas industry to provide complementary seismic images for a better characterization of the subsurface. With the introduction of converted-mode (PS-down primary and up shear travelling waves) seismic methods, the ability to solve complex geological problems is on the rise. In areas where traditional PP seismic surveys lose quality, such as gas clouds, thin bed lithology, and heavily fractured carbonate reservoirs, adding the PS seismic can better resolve the targets and increase the confidence in the seismic interpretations (Donati et al., 2016; Gupta et al., 2017; Triyoso et al., 2017). PS seismic data have advantage over traditional PP seismic data when imaging gas or fluid bearing formations. PP seismic signals tend to attenuate upon encountering gas/liquid bearing formations, leaving the seismic images with missing information (Triyoso et al. 2017). In contrast, the S-wave component of the PS seismic data is less sensitive to gas/liquid allowing a better image of gas/liquid bearing formations. Gas and fluids do not have a shear modulus; allowing the PS seismic data to image through areas of uncertainty due to gas clouds (Stewart et al., 2003).

PS seismic techniques have been around for more than twenty years. Technological advances made PS data acquisition and processing more attainable and more economical. Kristiansen et al. (2005) have successfully used multicomponent seismic data (PP-PS) in identifying fractures within carbonate reservoirs. PS methods have an advantage over conventional PP fracture characterization techniques due to the shear wave splitting property of the PS data (Crampin, 1985). Once a shear wave encounters a fracture, the wave splits into two directions, one moves in a direction parallel to the fracture and the other moves perpendicular to the fracture (Kristiansen et al., 2005, Fig. 1). Shear wave splitting provide information about the fracture's orientation and density, which is a primary application of PS data in fracture characterization (Chopra et al., 2019). However, because PS data is often noisy, and difficult to analyze and interpret, in many cases the co-acquired PS data may not be fully utilized (Gupta and Hardage, 2017). Despite the significant improvement in the PS data analysis and interpretation, adding PS data to every conventional PP seismic exploration project is still far from being achieved.

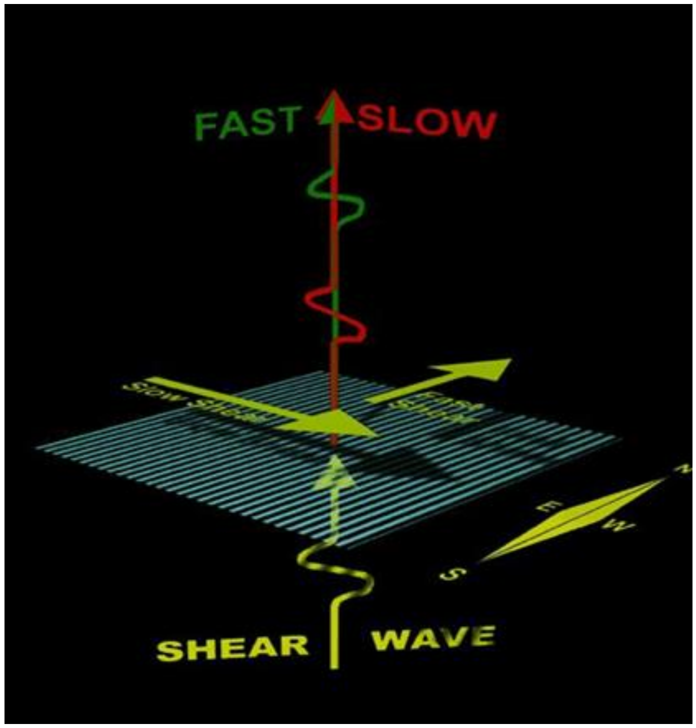

Figure 1 An image shows shear waves splitting as they encounter a fracture. The fast shear moves parallel to the fracture, while the slow shear component moves perpendicular (after Chenin and Joyce, 1999).

This study aims to expand the use of the PS seismic data in characterizing fractures in the Mississippian carbonates. PS fracture characterization is based mainly on shear wave splitting analysis. However, a new workflow that generates and integrates multiple attributes of the processed PS seismic volume is tested in this study as new PS seismic-based fracture characterization approach. This workflow was adopted by a recent study by Bedell (2019) for PP-seismic based fracture characterization within the same geological intervals investigated in this study. The intent is to expand the use of PS data for fracture characterization and compare to PP data as a means to better understand the reservoir. A detailed comparison will be made between the fracture characterization results attained from PP, PS, and combined PP-PS results.

CHAPTER II

GEOLOGIC BACKGROUND

The study area is located in central Oklahoma within the STACK (Sooner Trend Anadarko Canadian and Kingfisher counties) Play (Fig. 2). The Devonian Woodford Shale and the Mississippian carbonates “Meramec and Osage” are the primary targets for exploration. The Woodford Shale is an organic-rich shale, characterized by its dark gray to black color, phosphate nodules and pyrite (Cardott et al., 1993). A very important aspect of the Woodford Shale is its Total Organic Carbon (TOC) content of up to 25 percent as well as type II kerogen (Comer, 1992). Due to the kerogen type and high TOC content, the Woodford Shale provides an excellent source rock for the overlying Mississippian carbonates, which have been the target reservoir since the discovery of the play. The Mississippian carbonates characterized in the study are the “Osage and Meramec” intervals. Osage is an operational term often used to describe cherty carbonate at the base of the Mississippian interval believed to be Osagean in age. Meramec is another commonly used operational term used to refer to the limestone dominated interval between the “Osage” and the “Chester Shale” (Stukey, 2020). The “Osage limestone” was deposited in the early Mississippian, whereas the “Meramec limestone” was deposited during the Middle Mississippian. The “Osage and Meramec” intervals have proven reservoir quality and provide a unique benefit when drilling these “stacked” reservoirs by providing multiple potential pay zones. Several key factors contribute to the success of the STACK play including hydrocarbon type, maturation, as well as source rock burial depth (Welker et al., 2016).

During the Early Mississippian, much of Oklahoma was covered by a shallow seaway in a subtropical environment (fig. 3). The depositional environment has been classified as a distally steepened ramp, dominated by wave action, indicated by high sediment production and dispersion (Wang et al., 2019; Childress and Grammer, 2019; Price and Grammer, 2019). The "Osage limestone" as a whole was characterized into Lower and Upper Osage intervals Wittman (2013). During deposition of the "Lower Osage", sea level was higher, resulting in a less oxygenated environment with low sedimentation rates. During deposition of the "Upper Osage", carbonate production increased, keeping up with sea level rise and subsidence rates (Wittman, 2013).

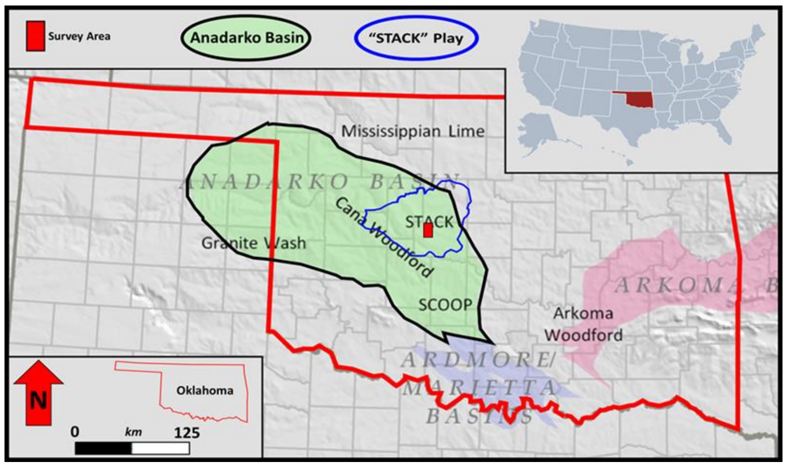

Figure 2 Location of the study area, (from Bedell, 2019; modified after IPPA, 2018)

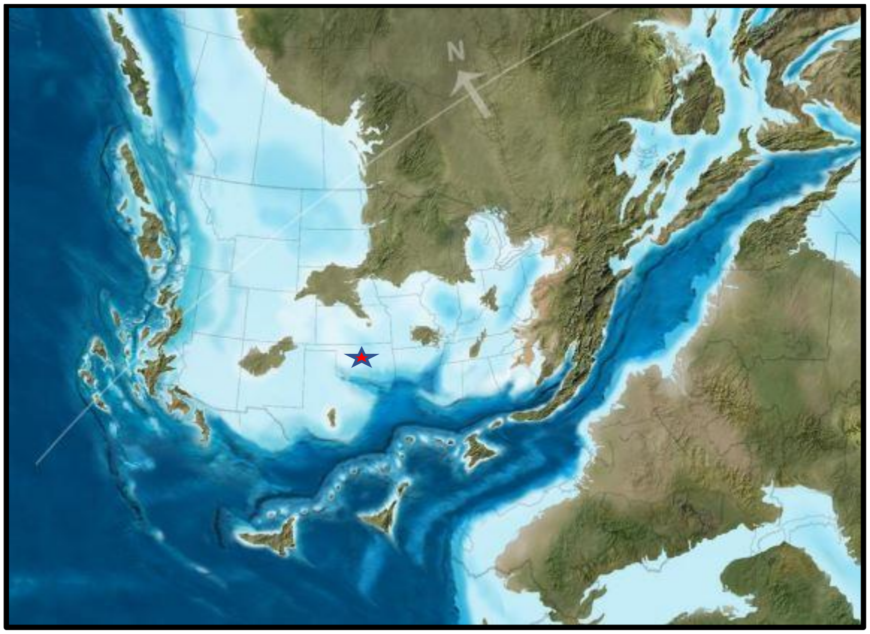

Figure 3 Paleogeographic location of Oklahoma during the Early Mississippian (~345 Ma) the star represents the location of the study area (modified after Blakey, 2013).

A transgressive sequence is seen as the “Meramec limestone” was deposited, overlying the “Osage limestone”. Like the “Osage limestone”, the “Meramec limestone” was characterized into Lower and Upper intervals based on specific petrophysical log signatures. While the “Meramec limestone” contains several small coarsening upward packages, the overall character of the formation is a fining upward sequence containing large amounts of clay particles. This increase in clay relates to higher porosity than what is found in the “Osage limestone” (Droege et al., 2018). The “Lower Meramec” is characterized by heavily bioturbated calcareous siltstone with intergranular porosity and calcareous fossil fragments, rounded peloids and quartz within this interval (Droege et al., 2018). The “Upper Meramec” was deposited during a time of increased sedimentation and as a result, the total thickness of the “Meramec limestone” in the study area is more than 121 meters (397 feet). The rate of sedimentation was sufficient to surpass sea level rise and the subsidence rate, allowing carbonate production to fill available accommodation space (Wittman, 2013).

Tectonically, the STACK play is located on the Anadarko Basin shelf. The Anadarko Basin dips southwest and at its deepest point is in excess of 12192 meters (~40,000ft) (Patel et al., 2021; Perry, 1989). Perry (1989) divided the tectonic evolution of the Anadarko Basin into four distinct stages: (1) In the middle Proterozoic, crustal consolidation and metamorphism was taking place during a time when igneous activity started to form the basement rock in what is now central Oklahoma, (2) During the Cambrian Period, the Southern Oklahoma Aulacogen was developed, (3) The development of the southern Oklahoma trough from the Cambrian to the Mississippian times, and (4) Late Mississippian to Pennsylvanian subsidence and uplift as the present intracratonic foreland basin formed. The Anadarko Basin is bound to the south by the Arbuckle uplift, the Amarillo-Wichita uplift to the southwest, the Nemaha uplift to the east, and thins to the north as it approaches the Central Kansas uplift (Gay, 2003) (fig. 4). Gay (2003) indicated the Nemaha uplift is structurally similar to the Rockies, and developed as the result of compressional tectonics.

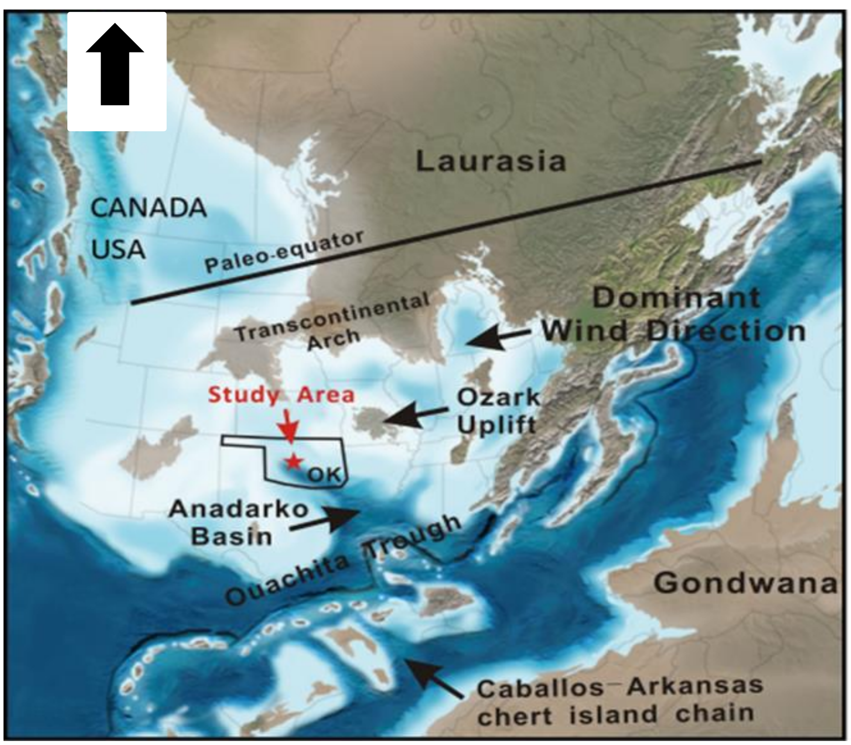

Figure 4 Study area shown bound by major structural features (modified from Wang et al., 2019, after Blakey, 2013).

The Nemaha uplift, which resides directly east of the STACK play, is characterized as a large listric thrust fault with shallow dip angles within the basement rock and moves into near-vertical to vertical dip as it moves through younger stratigraphic units (Gay, 2003). Strike-slip movement is associated with the Nemaha uplift and is believed to be related to later thrusting events (Gay, 2003; Mcbee, 1999; Berendsen and Blair, 1992; Blair and Berendsen, 1988; Davis, 1986).

CHAPTER III

DATA AND METHODOLOGY

3.1 DATA

Data used in this study were donated by Devon Energy Corporation and consist of processed three dimensional multicomponent seismic (3D3C) surveys and one well with a full suite of logs. The well is located within the area where both PP and PS surveys overlap and were used to tie the PP data to well data for ground truthing. Devon also provided horizons to aid in the registration process and were used before the PP-PS fracture characterization began. The PP seismic survey covers a larger area than the PS seismic survey. However, this study is limited to the area where the PS survey overlaps the PP survey (Fig. 5), which has a surface area of 65 km^2 (25 mi^2). Both PP and PS seismic volumes have a sampling interval of 2 ms and were processed and imaged using orthorhombic migration scheme.

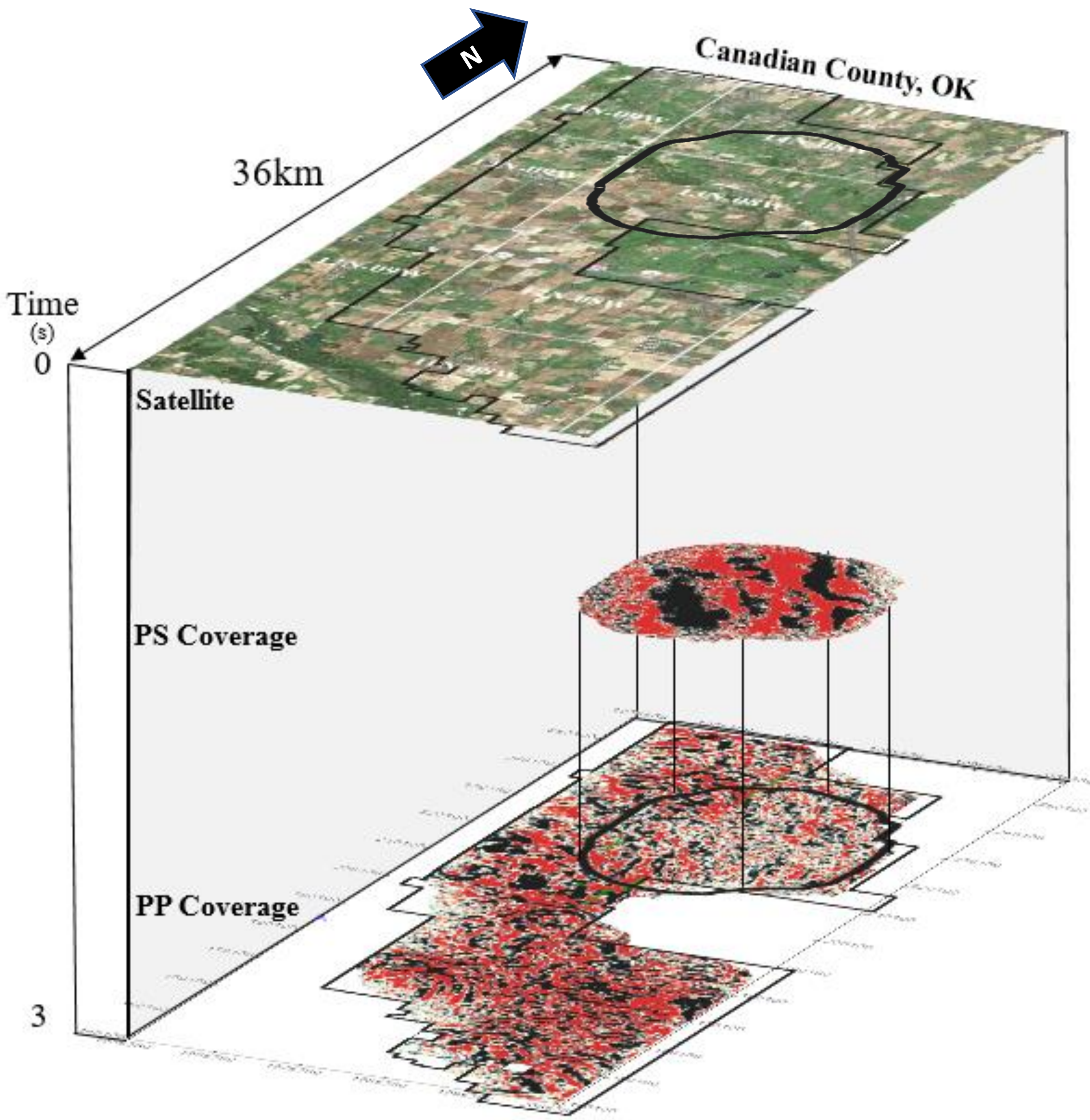

Figure 5 Oblique view of the seismic survey. The top image is a satellite photo showing the location of both the PP and PS survey areas within Canadian County. The middle image is the coverage of the PS survey, and the bottom image is the PP coverage. Outlines of both the PP and PS surveys can be found on the satellite image.

3.2 METHODOLOGY

A thorough review of literature was conducted in order to develop a better understanding of the stratigraphy, tectonic background, and how the use of PS seismic can improve fracture characterization. Understanding the depositional processes of the Meramec and Osage stratigraphic units aids in determining where the more heavily fractured zones may appear. A seismic based fracture characterization to help identify large- and small-scale fractures was conducted using the PP and the PS seismic data separately. The workflow developed by CGG's *InsightEarth* Software (Bedell, 2019) for seismic characterization of fractures was adopted in this study. The following processing steps were completed as part of the seismic characterization of fractures workflow:

3.2.1 Well to Seismic tie

The PP and PS seismic data were first loaded into CGG's HampsonRussell program for the initial well ties. The horizons were loaded from the previous PP study and quality-controlled to ensure accuracy.

The well-to-seismic tie was first completed for the PP seismic data. This well tie provides a link between the seismic waves and true subsurface geology, which in turn, provides a more accurate interpretation. When creating the synthetic seismogram to be used in the well tie, sonic and density logs were used to create the reflectivity log. The reflectivity log was then convolved with a wavelet extracted from the seismic data with the addition of random noise as seen in equation 1 (Cubizolle et al. 2015).

$$s(t) = w(t) * r(t) + n(t) \qquad 1$$

Where s(t) is the synthetic trace, w(t) is the wavelet to be convolved with the reflectivity log (r) defined by sonic and density curves from the well logs, and n accounts for random noise that may be in the data.

Once the synthetic seismogram was created, it was compared to real seismic data and a bulk shift was applied, as needed, to match the synthetic seismogram to corresponding seismic reflectors. After the bulk shift was applied, stretching and squeezing of the synthetic was necessary to properly align important formation markers. This alignment helps in updating sonic velocity and drift times attained at higher frequency (normally in kilohertz), so that it matches seismic acquired at lower frequencies (in hertz) to remove the effect of dispersion (fig. 6). A well tie was not created with the PS data. Once the PP data was tied to the well, the registration process took place to properly align the PP-PS.

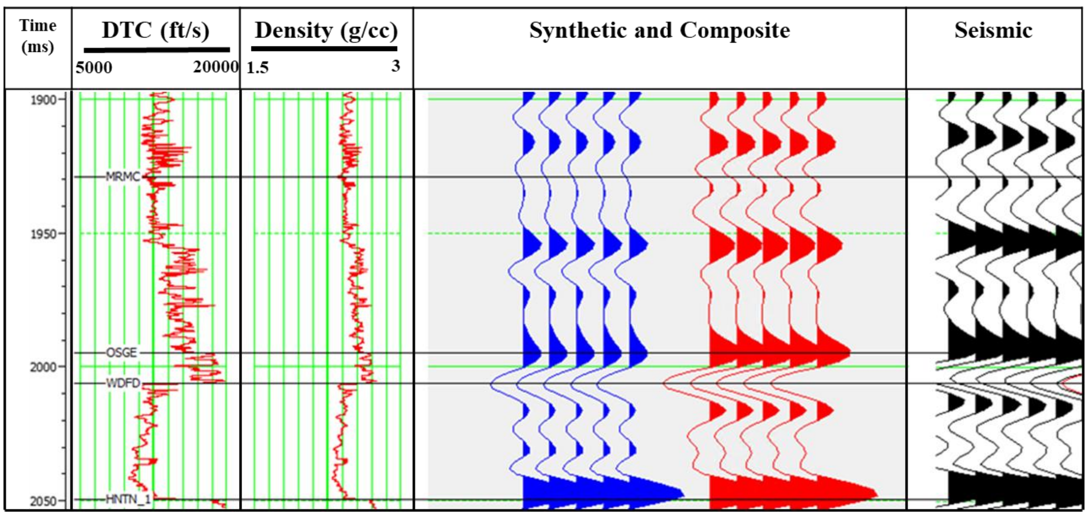

Figure 6 PP well-to-seismic tie to constrain the seismic horizons for interpretation and the PP-PS registration process correlation factor of 93 percent ensuring a quality well tie.

3.2.2 PP-PS Registration

Before a detailed interpretation can be made on the PS seismic data, it must first go through a process called PP-PS registration. Registration is a process that corrects the travel time differences common with converted mode data (Chopra et al., 2019). The difference in time originates from the converted shear wave after it reflects off an interface or horizon. Since the shear waves travel slower than primary waves, the time at which subsurface structures appear in the PS survey will occur at a later time (fig. 7a). For the purpose of this study, a process called "Event Matching" was followed in order to register the data. Event matching is a process by which several geologically interpretable events (horizons) are picked in both the PS and PP volume based on the interpreter's discretion. For this study, horizons for the registration process were provided by Devon Energy and imported into *HampsonRussell* where one additional horizon was picked in PP and PS at a lower depth to complete the registration process. The horizons were evaluated before using them in the event matching process to minimize errors in the data registration. After correcting for small time shifts between PP and PS, the registered data (Fig. 7b), was imported into *InsightEarth* where the fracture workflow started.

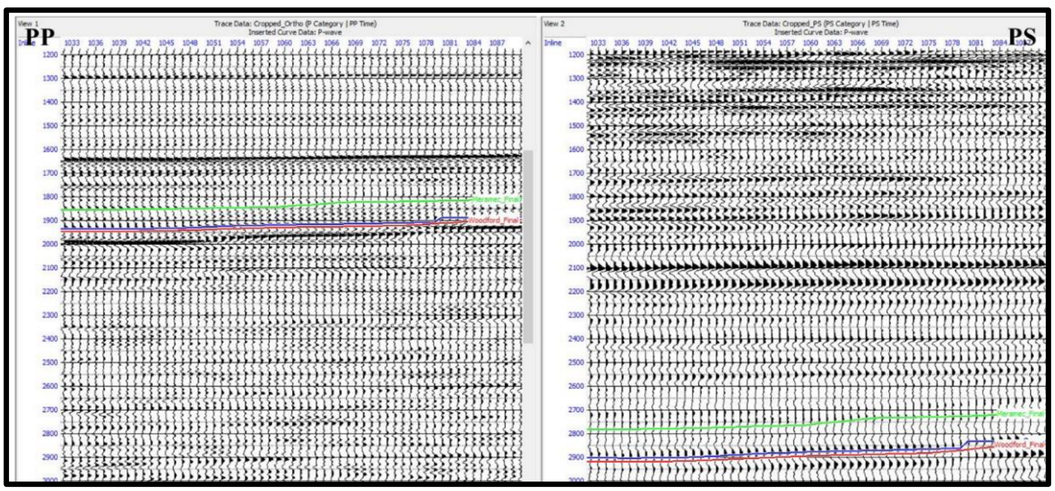

Figure 7a PP (left) and PS (right) seismic data before registration.

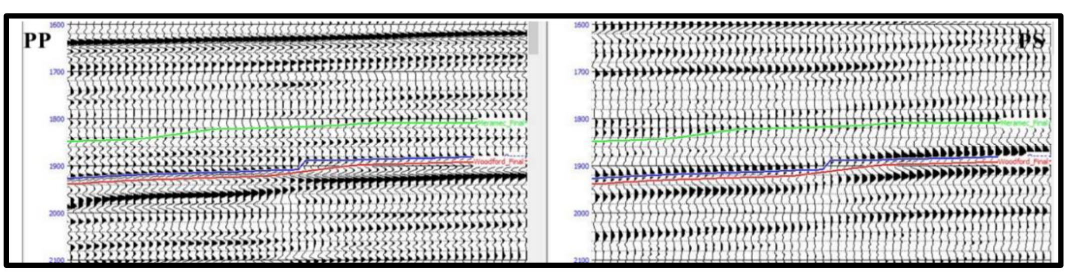

Figure 7b PP-PS post registration with a zoom in on the target horizons.

3.2.3 Data Conditioning

In order to attain the best fracture characterization results, the PS seismic data were first conditioned within *InsightEarth's* Ignition module. This process started by creating a Horizon Orientation volume from the original amplitude data. The Horizon Orientation volume preserves steeply dipping features within the seismic data, which is imperative to help characterize any fractures with near vertical dip angles. The next step was to use the original amplitude volume and the horizon orientation volume as inputs for the footprint removal process. The footprint removal process uses a measuring tool to determine the wavelength based on whether the footprint is axis aligned (crossline or inline) or oblique to the inline and crosslines. Since the acquisition footprint was very shallow and the area of interest lies at around 2000 ms, only one iteration of the footprint removal process was needed for the PS data. No conditioning steps were completed on the PP data as it did not produce the quality of fractures needed. After the footprint was effectively removed in the PS data, random noise was removed using a median statistical filter and care was used when applying this filter so that any fracture information was not removed during this process. A 3x3x1 median filter was applied during the statistical filtering application. A time slice at 650 ms in figure (8) shows the process of applying each filter and indicates the improvement in data quality with the elimination of the footprint. After the data conditioning process was complete, a fault extraction workflow was started.

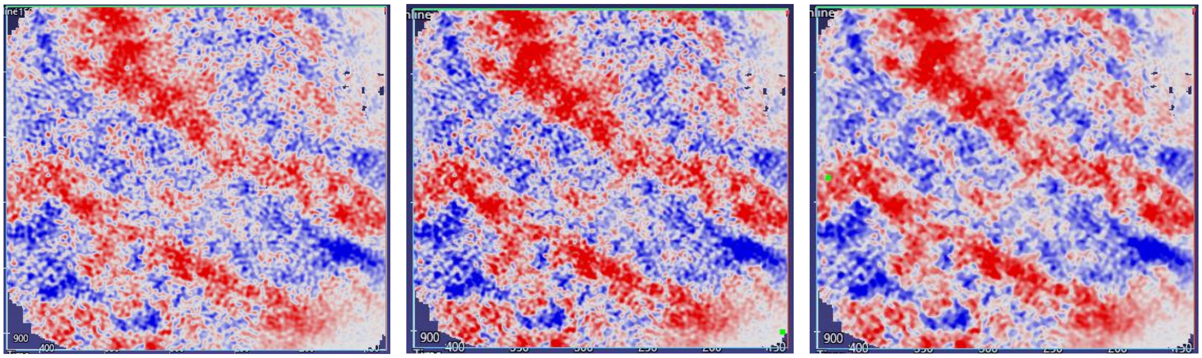

Figure 8 Time slice at 650 ms showing the original data (left panel), data after footprint removal (middle panel) and data after statistical filter applied (right panel).

3.2.4 Large-Scale Fault Extraction

The large-scale fault information such as strike and dip were extracted by the software using a series of attributes. Initially, attributes used for edge detection and various other curvature class attributes were generated to have an idea about fault structure in the study area. Visualizing the large-scale fault framework aids in the tectonic analysis through looking at differing stress/strain relationships. After the edge detecting and coherency attributes were generated, a process called Automatic Fault Extraction started automatically to pick faults, reducing false interpretations of faults caused by human errors.

Once the seismic data was conditioned through the Ignition module of *InsightEarth*, fault interpretation steps within the FaultFractureSpark module were started. This process started with creating an edge stack with a horizon orientation volume to get rid of artifacts caused by steeply dipping horizons that may get misinterpreted as faults. The edge stack creates a volume that highlights discontinuities and is used as an input when moving on to the Advanced Fault Enhance (AFE) steps. The AFE creates fault enhance, strike, and dip volumes through three different stages. The first stage is to create a strike enhance volume using the edge stack made previously. In this step, the edge stack is used to count the "voxels" or pixels to measure the thickness of faults in several representative areas. The strike-enhance volume contains the strike information of all faults to be identified and preserves the information for the third and final step. The dip-enhance volume is the next stage to run. To run this step, the amplitude volume is needed to analyze several inlines and crosslines and measure the angle of several faults to get a range of dip angles. The final stage is the fault-enhance stage where information from the strike and dip enhance volumes are compiled together to provide a more accurate representation of the fault framework in the seismic data. The dip-enhance volume is used to identify the “noise threshold” by adjusting the histogram so that enough good fault signal is present without adding in additional noise. Once the fault-enhance stage is completed, it is used as an input to create fault point sets by taking all the strike and dip information from the AFE stages and creates fault cuts, which then are clustered together based on strike and dip tolerances. Once the fault clusters have been generated, some manual picking was necessary to complete the faults extraction before converting the fault clusters to surfaces (fig. 9).

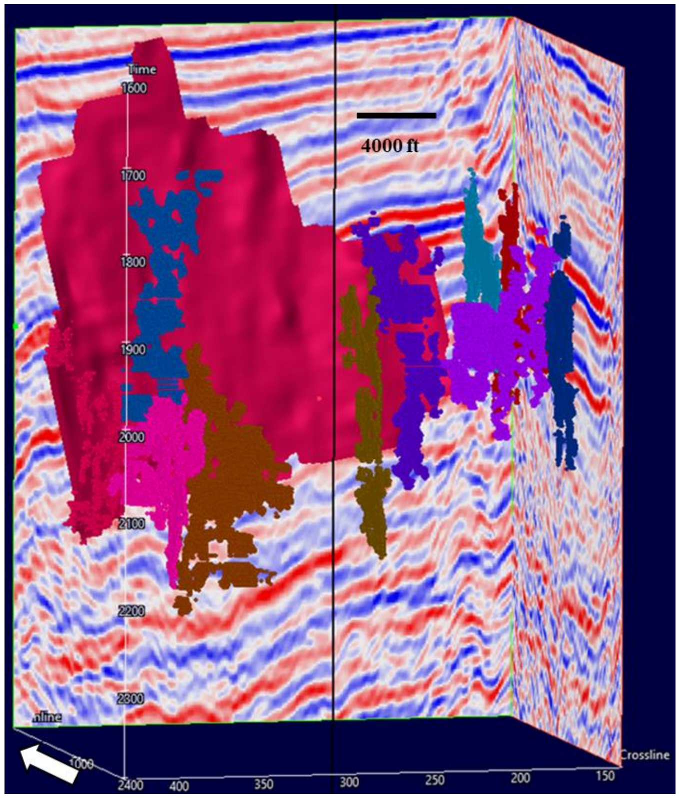

Figure 9 Large-scale fault framework. Strike and dip information is collected into point sets and clustered together to represent fault surfaces.

3.2.5 Curvature Class Attributes

After the large-scale fault extraction process on the PS volume was completed, the steps to create a DFN were completed to reveal small-scale fractures. Six curvature class attributes were created as a starting point for the DFN. These attributes include K1 and K2 (used as inputs for the other four attributes), Mean, Gaussian, Most positive, Most negative, and their associated azimuths. The K1 attribute is used to highlight anticlinal and domal features, where the K2 attribute is useful for the opposite, such as synclinal and bow features (da Silva et al., 2014) (fig. 10).

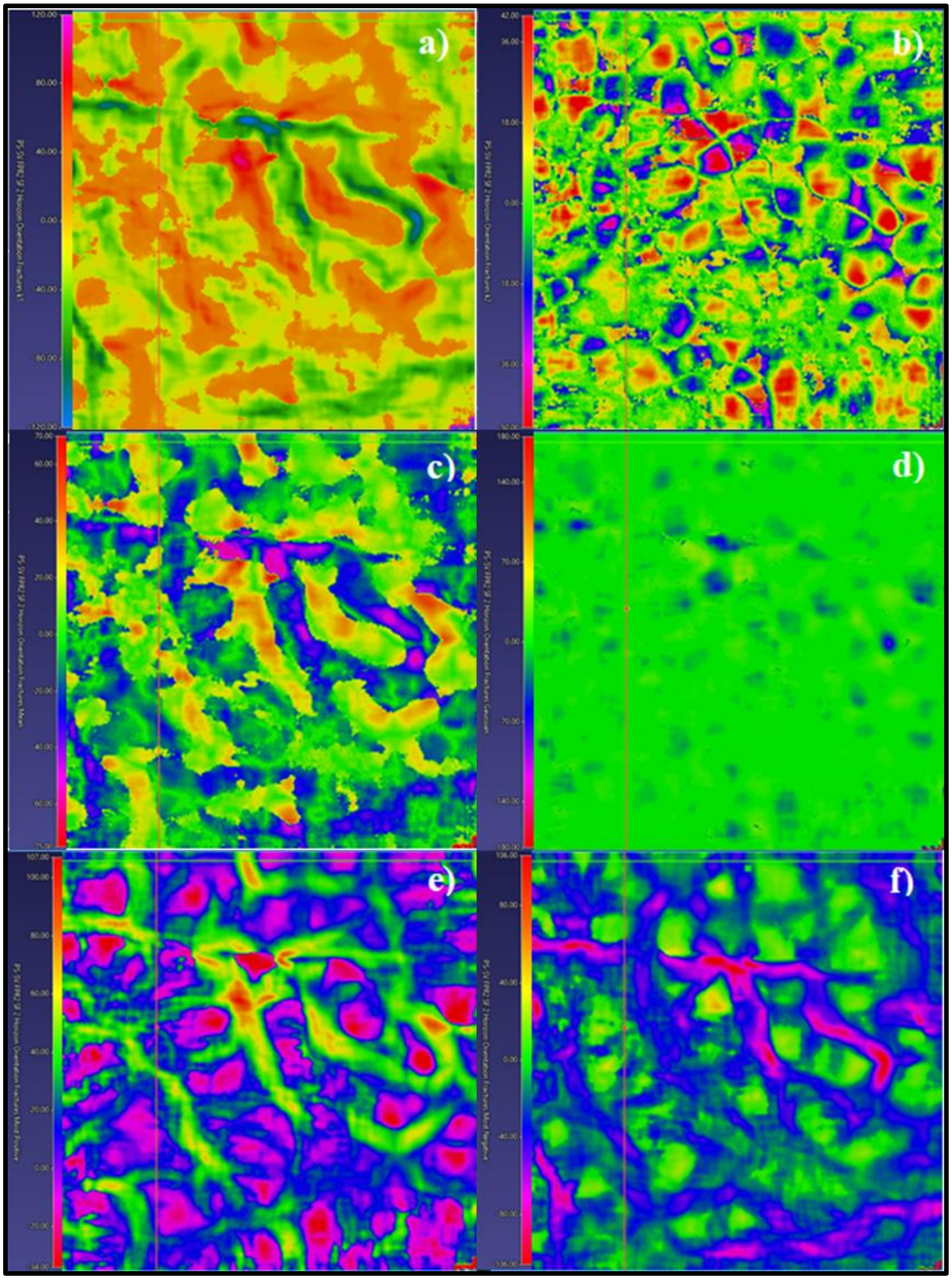

Figure 10a-f Attributes generated from K1 and K2 using "InsightEarth". A) K1 attribute is useful to identify anticlinal and domal features. B) K2 attribute is most useful in identifying synclinal features. C) Mean curvature is similar visually to maximum curvature; however, it is used to develop other curvature class attributes. D) Gaussian curvature is most useful when applied to a mapped surface, it is best used in producing other curvature attributes. E) Most positive curvature searches normal curvatures and looks for the most positive values. F) Most negative curvature shows the opposite and looks for the most negative values within normal curvature (Roberts, 2001).

3.2.6 Discrete Facture Network (DFN)

After the attributes were generated, the same steps used for large fault extraction were applied to build the DFN after adjusting the parameters to better detect small scale fractures. Building the discrete fracture network involved three steps. The first step estimates strike information, which is used as an input to the second step for extracting the dip information. The final step uses both the strike and dip information as inputs to provide a fracture enhanced volume highlighting fractured zones. The point sets containing fracture information obtained from the first three steps are used in another process to model the visible fractures (fig. 11). The final step was to add what are called *"glyphs"* (fig. 12). These glyphs are used to characterize fractures that are not seen by the naked eye and use vectors to show fracture magnitude and orientation.

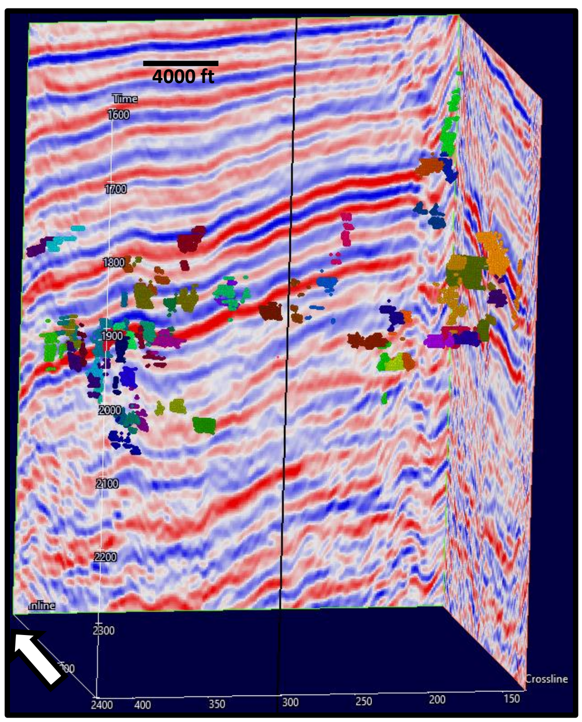

Figure 11 A side view of the generated discrete fracture network.

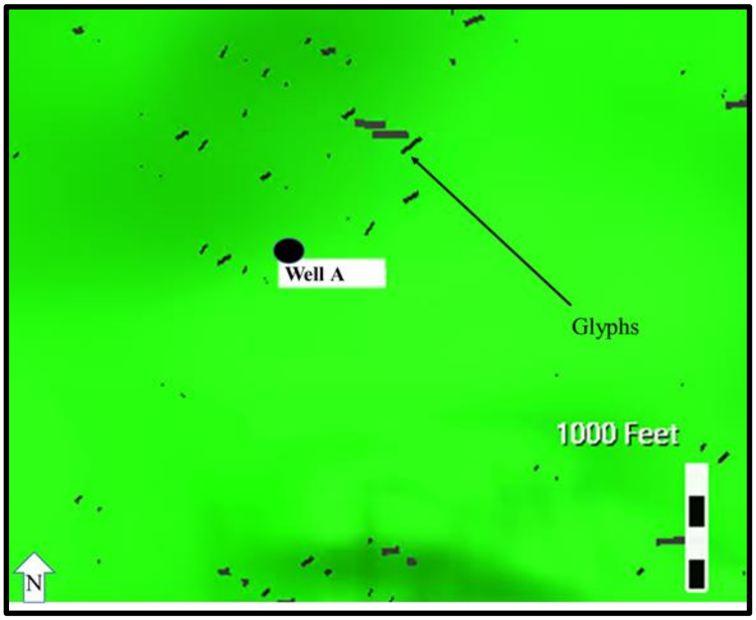

Figure 12 An image showing "glyphs" generated from fracture strike orientation attributes and used to represent fracture orientation and magnitude below seismic resolution.

3.2.7 Comparing fractures from the PP and PS data

After the PP and PS seismic fracture characterizations of fractures were completed at the study site, it was necessary to compare the results from both data sets. Comparing the results included evaluating the generated attributes, large-scale fault structures, and ultimately comparing the DFN of both PP and PP data. Based on this comparison, it was possible to evaluate the efficacy of fracture characterization by the PP and the PS data sets.

CHAPTER IV

INTERPRETATION

Although processing the PP and PS seismic data was completed in this study, this chapter focuses only on the interpretation of the PS seismic data. The next chapter will elaborate on comparing the seismic fracture characterization from the PS and the PP seismic data.

4.1 PS INTERPRETATION

The PS seismic data was interpreted to map and characterize fractures within the Mississippian Meramec and Osage intervals. Interpretations included the stratigraphic horizons of the Meramec, Osage, and Woodford Shale, respectively to constrain fracture interpretation (Fig. 13). The green horizon is interpreted as the top of the Meramec while the blue horizon is interpreted as the top of the Woodford and is used to display the bottom of the Osage limestone. The interpreted horizons constrain the upper and lower limits of the interpreted fractures. Curvature and coherency class attributes were generated to aid in interpreting the location of fractured zones. A fracture highlight attribute was generated to help visualize areas where the highest likelihood of fractures was predicted to be found. The discrete fracture network (DFN) was built to visualize fractures in 3D space. Once the DFN was generated, the observed fractures were seen within the areas where the curvature attributes found the highest concentration of fractures to be present.

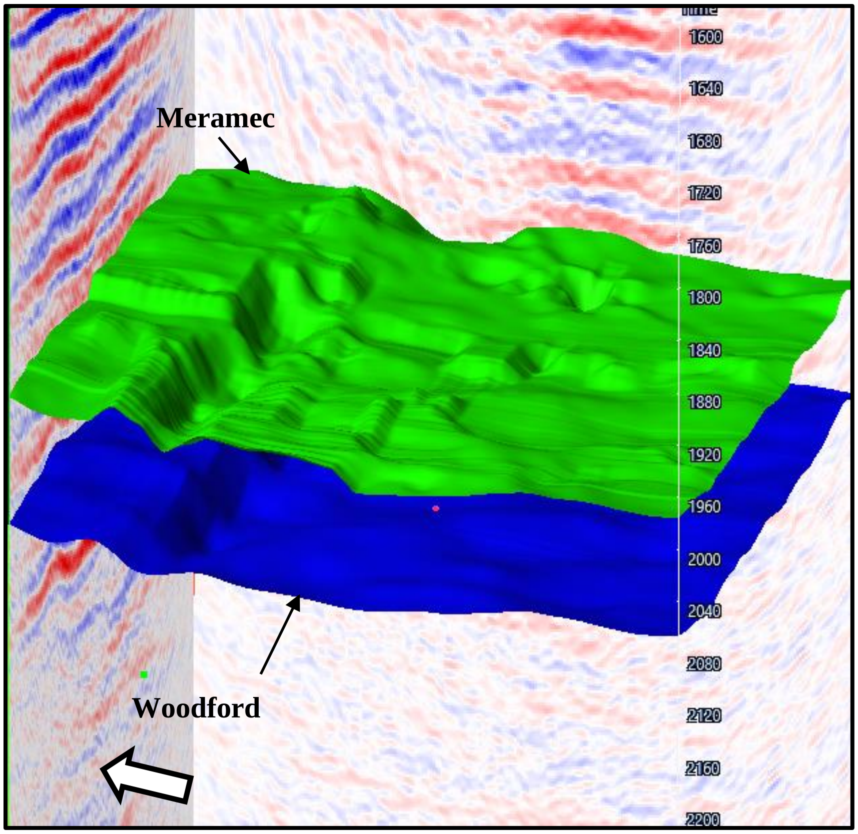

Figure 13 Stratigraphic horizons interpreted to provide constraint to the seismic characterization of fractures. The top horizon (green) is interpreted as the top of the Meramec interval. The bottom horizon (blue) is interpreted as the top of the Woodford, or the base of the Osage. The figure shows vertical displacement at the north end of the survey area. Interpreted as strike slip fault.

Understanding the structural framework provides information regarding the paleostresses in the area and insight into potential trends of fracture distribution. The Meramec and Woodford horizons show vertical displacement in the study area indicating offset caused by faulting (fig. 14). The discontinuity in the amplitude data is a clear indicator of faulting at this location. The large-scale fault framework shows a large East-West trending fault with a strike of ~90 degrees and a near vertical-to-vertical dip in the north end of the survey (fig. 15). The large fault located in the northern part of the image is interpreted as an oblique strike-slip fault indicated by the horizontal displacement and can be seen in the time slice image at 2000 ms within the amplitude data (fig. 15). In this time slice several other smaller E-W trending faults are observed that may indicate this was the dominant tectonic stress regime direction at the time the deformation occurred. The rose diagram generated to show the strike trends of the large-scale faults indicate the dominant strike to be ~85-90 degrees and the dip angle of all faults in this model shows 85-90 degrees (fig. 16).

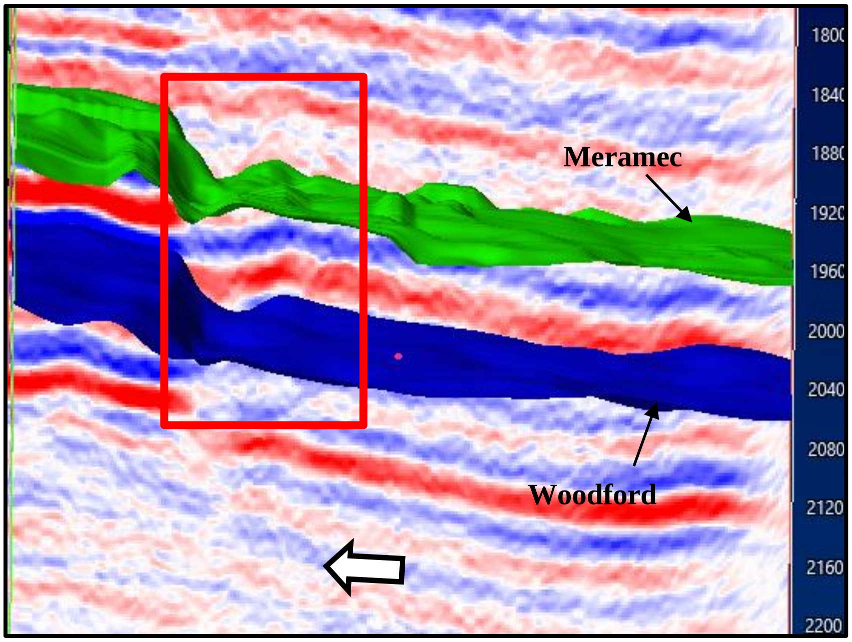

Figure 14 A closer look on the Meramec and Woodford horizons provides a better view of the vertical displacement (shown in the red box) associated with the large-scale faulting.

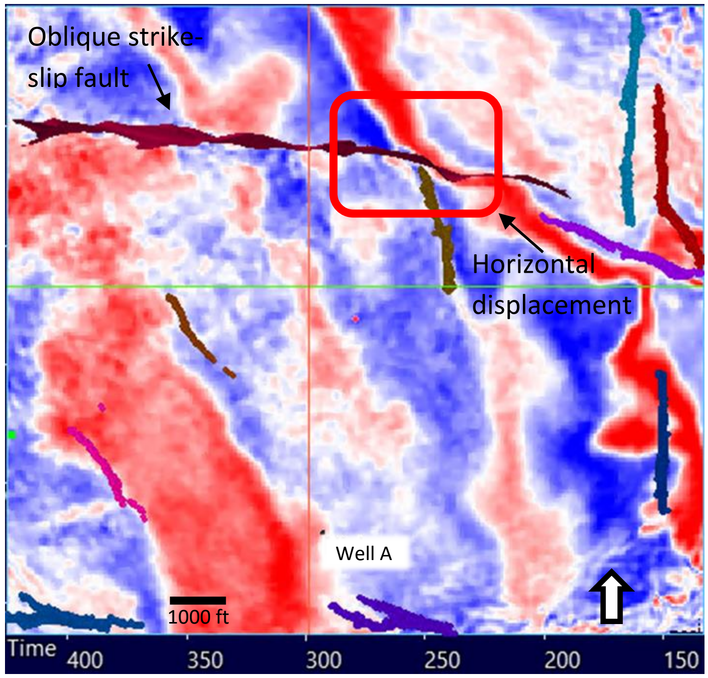

Figure 15 Time slice at 2000ms showing the orientation and magnitude of large-scale faults. Notice the large E-W trending fault showing horizontal displacement on the time slice.

Strike	Dip
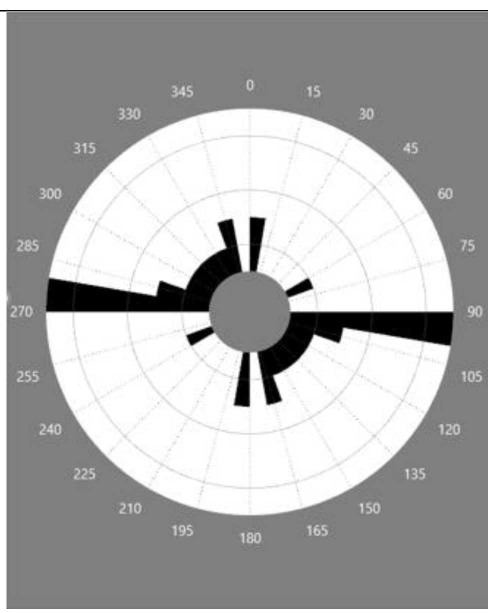	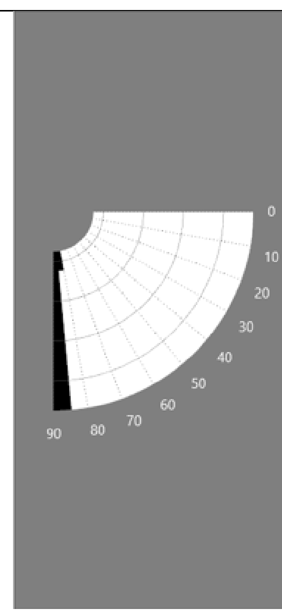

Figure 16 The rose diagram generated from the large-scale faults to show the dominant strike trend (left panel) and the dip angle associated with it (right panel).

Curvature class attributes such as Most Positive and Most Negative curvature provide the ability to visualize fault and fracture structure. The Most positive and Most Negative attribute generated helps identify both large faults and fractured zones by highlighting areas of the highest and lowest curvatures in the seismic data (fig. 17). Figure 17 shows the Most positive curvature attribute, where a large structural feature can be seen spanning the northern portion of the area and striking east to west. The westernmost area in figure (17) is interpreted as a highly fractured zone indicated by the increased curvature noted by the scale bar and the density of discontinuous features. The northeast area of the study area shows a small presence of fractures as indicated by the discontinuity, however, most of the features in this area are interpreted as larger-scale faults. In the southeast portion of the study area, the fractures are slightly more prevalent and there is a combination of large and smaller scale features (fig. 17).

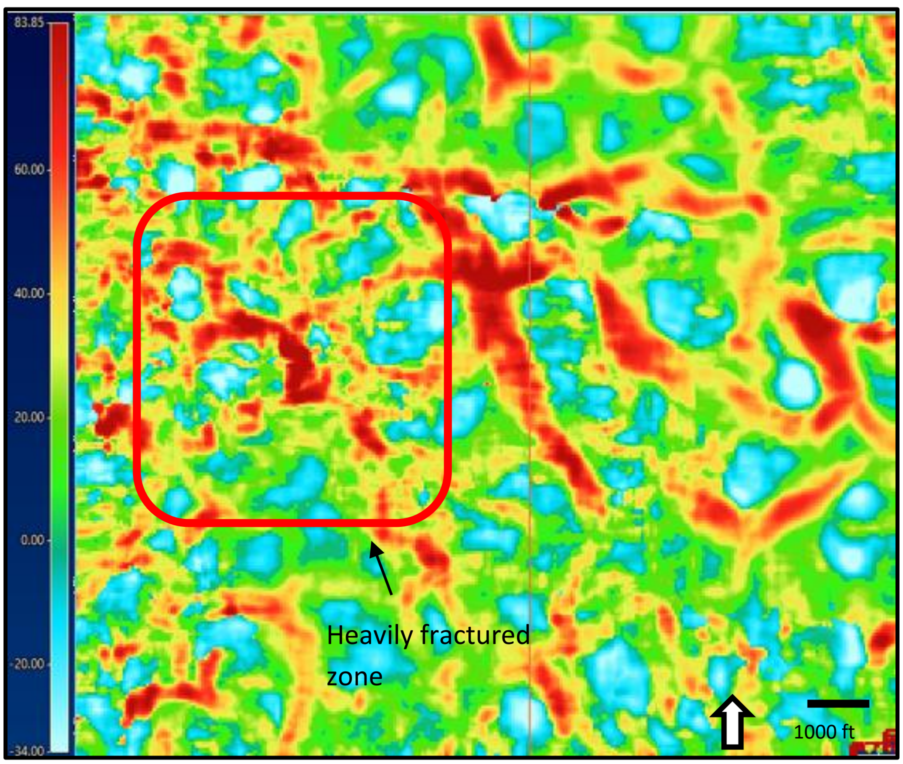

Figure 17 Most positive curvature attribute generated to show areas where increased curvature is present. A large continuous feature can be seen that correlates to the large-scale faults extracted in figure (15).

The generated Discrete Fracture Network (DFN) in figure (18) provides a 3-dimensional representation of how a particular formation of interest is fractured or deformed, to identify the potential fluid flow within the formation when planning a potential prospect. Faults and fractures provide a mode of secondary porosity and could increase production potential, especially in carbonates reservoirs. The DFN generated in this study represents "Mississippian limestone" intervals bounded from the top by the Meramec interval and from the bottom by the base of Osage interval (fig. 18). The fractures observed between the Meramec and Osage horizons were shown to include ones that intersect the upper and lower-most limits that show the potential migration of hydrocarbons. Most extracted fractures directly correlate to the highly fractured zone seen in the Most Positive Curvature attribute with a dominant strike trend of ~90-120 degrees. A secondary strike trend exists at ~140-160 degrees that can be interpreted based on the different stress trends. The dip angle of the observed fractures is similar to the larger-scale faults lying between ~70-90 degrees, which is expected since the fractures are present within the same formation interval. A time slice taken at 2000 ms and its associated rose diagram provides a bird eye view of the fractures (Fig. 19). The majority of the fractures are located in the westernmost region of the study site. The dominant orientations of the fractures correlate well with fracture orientation identified by the shear wave sonic dipole-dipole log located at the southern end of the study area. The rose diagram generated from the dipole-dipole sonic log shows a strong strike trend of 150 degrees, confirming the results of the seismic data analysis (fig. 20).

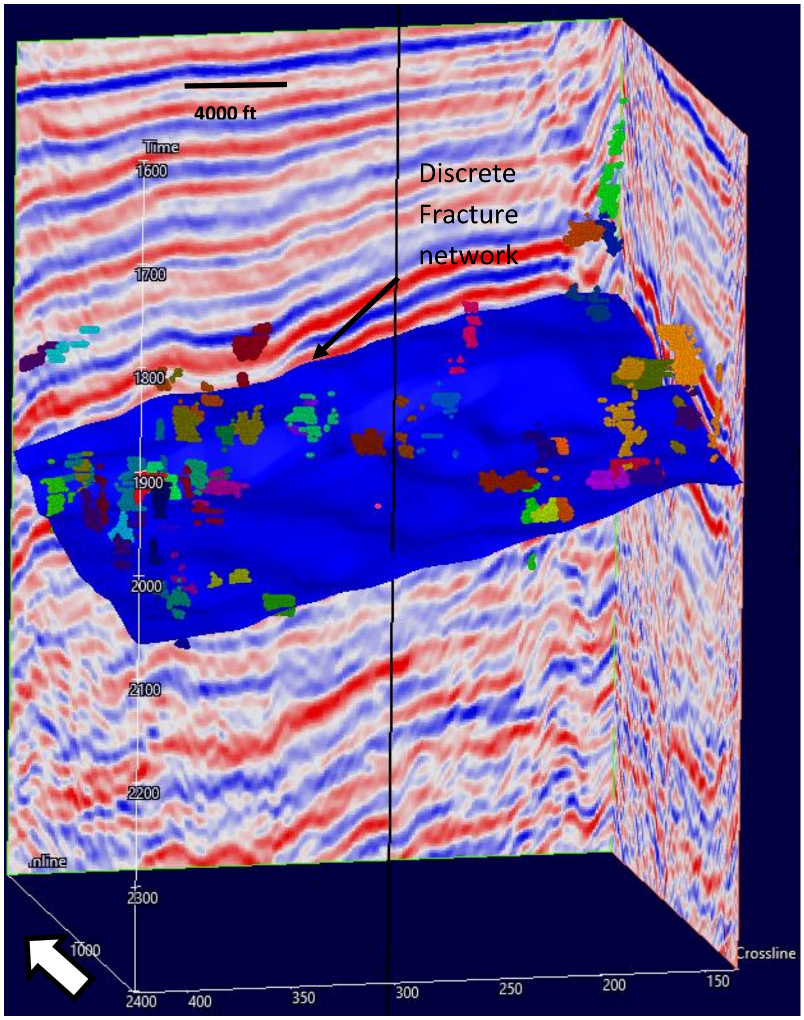

Figure 18 3-D representation of the DFN within the Mississippian Meramec and Osage intervals showing all fractures within the area of interest and fractures that intersect the boundaries of the formations.

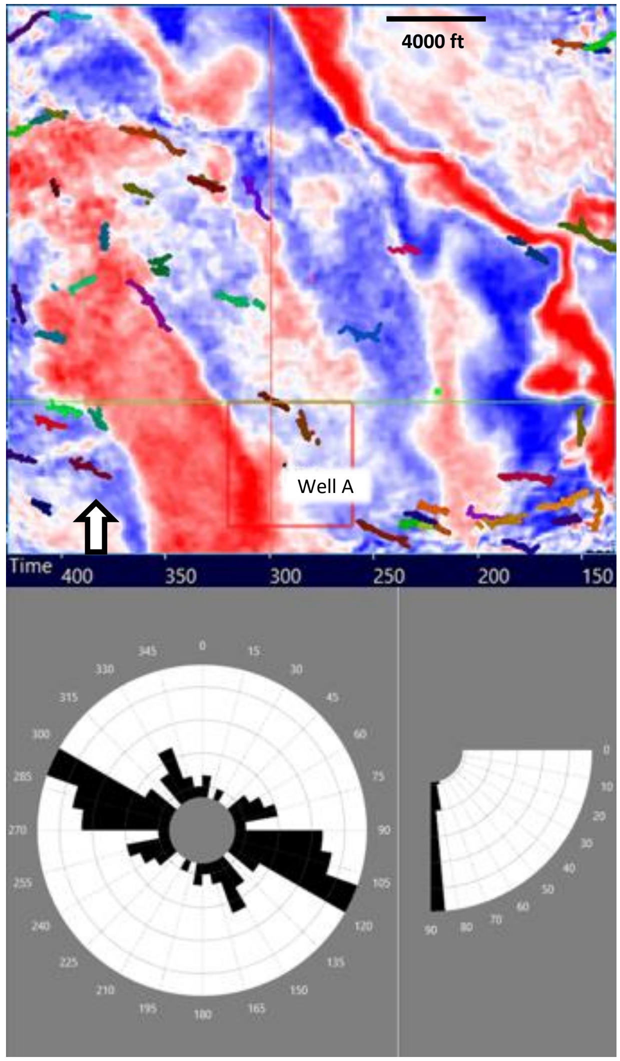

Figure 19 a) a time slice taken at 2000 ms with fractures locations and orientation indicated, and b) a rose diagram generated from the fractures shown above.

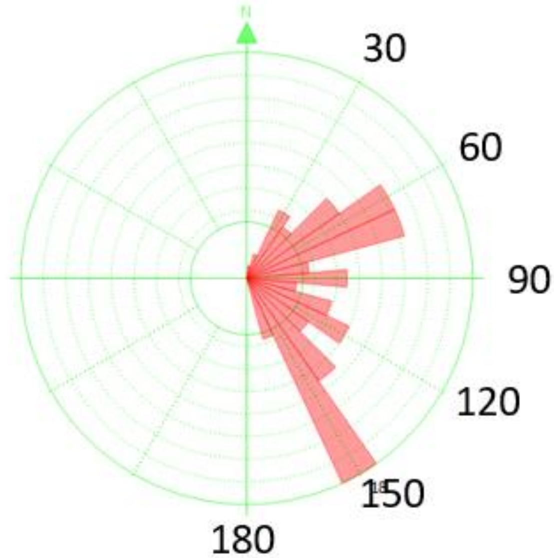

Figure 20 Rose diagram of fractures detected using the dipole-dipole shear-wave sonic log (Well A) showing the most dominant strike of fractures to be ~150 degrees. This rose diagram shows good correlation to the fractures extracted within the seismic data near the wellbore. It is important to note this information is from a single well and comes from one representative area in the seismic data.

4.2 COMPARING THE SEISMIC FRACTURE CHARACTERIZATIONS FROM THE PP AND THE PS DATA

The PP seismic data considered in this study is a part of a larger seismic volume that was processed and interpreted by Bedell (2019). The primary goal of this study was to conduct a PS seismic characterizations of fractures and compare it to the previous PP study. However, the preliminary comparison indicated that the PS seismic data shows unreasonably more fractures than PP data, which necessitated reviewing the processing sequence of the PP data. Using unconditioned (without filters) PP seismic data as input to the fracture characterization workflow results in better fracture characterization than using conditioned data. Therefore, the PP seismic data were reprocessed using the existing horizons and well data prior to comparing it to the PS data. Reprocessing the PP seismic data included seismic-to-well tie using one well with full log suites containing P and S sonic logs, density logs, and cross-dipole shear logs with azimuths

Comparing the PP and PS seismic interpretation begins with the large-scale structural comparison between the two datasets. In order to establish a relationship between the PP-PS data, the large-scale faults were compared to determine how closely the data compares. The most notable feature shown in both PP and PS is a large E-W trending fault described by Bedell (2019) to be a left-lateral oblique strike-slip fault (fig. 21). Figure (21) indicates the strike trend of this fault found in both datasets to be ~95 degrees. Upon further examination of this figure, one can notice another smaller fault just to the southeast of the large E-W fault. The good correlation of major fault interpretations increases the confidence that the PP and PS data image similar structures. Although there are similarities, differences occur elsewhere in the example PP and PS time slices shown in figure (21). In the PP data, there are dominantly NE-SW trending faults whereas in the PS data, the remaining faults tend to trend more NW-SE. However, the rose diagrams shown in figure 21, indicate that the fractures orientations seem to be very similar.

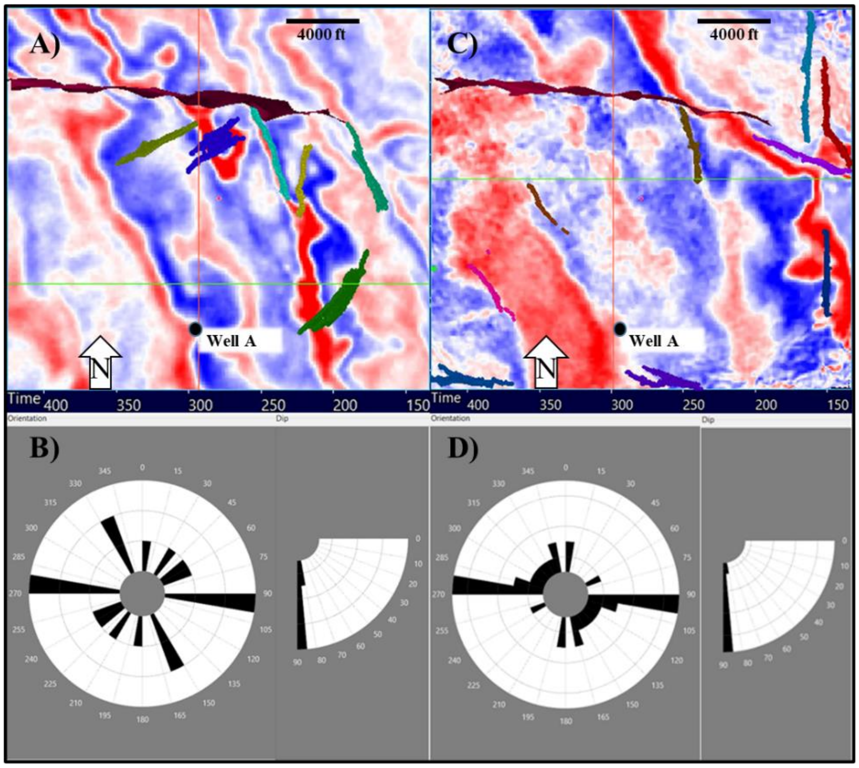

Figure 21 A) Time slice taken at 2000 ms in the PP data showing large-scale fault system. B) Rose diagram of PP faults showing the orientations and dip angle of the data. C) Time slice of PS data taken at 2000 ms, this figure varies slightly from the PP data, but shows some similarities. D) Rose diagram of extracted faults found within the PS data to show strike and dip angles.

The reprocessed unconditioned PP volume was used to extract fractures and create the DFN within the Meramec and Osage intervals. This yielded results with the highest concentration of fractures seen in the western and easternmost areas with very few fractures imaged in the center of the data. Fracture distribution from the PP varies slightly from the PS data where the highest concentration of fractures is located in the westernmost area of the survey (fig. 22). The orientation of the visible fractures varies slightly between PP and PS data. Similar to what is shown in the larger scale fault extraction, the small-scale fractures in the PP trend more in the NE-SW direction, whereas the fractures recognized in the PS data trend dominantly in the NW-SE direction. There is some overlap in the strike direction in the PP and PS data where most of the distribution and orientation of smaller fractures agree. The strike trend between 90-120 degrees is visible in both datasets according to the rose diagrams located in figure 22. The PP data shows a strong fracture trend at 60 degrees, which is imaged by the PS data but not as significant as in the PP data. The most dominant fracture trend characterized by the PS data ranges from 90 to 120 degrees, which is also characterized, but not as prominent, by the PP data. Additionally, both PP and PS data show a fracture trend at 150-degrees but is slightly more significant in the PS data (fig. 22). Figure 22a shows a series of fractures located in the southwest corner of the PP data striking in the 150-degree direction, which is also seen in other areas by the PP data. Figure 22b shows similar fractures located in the southwest corner of the PS data that directly compare to the 150-degree trend seen in the PP data.

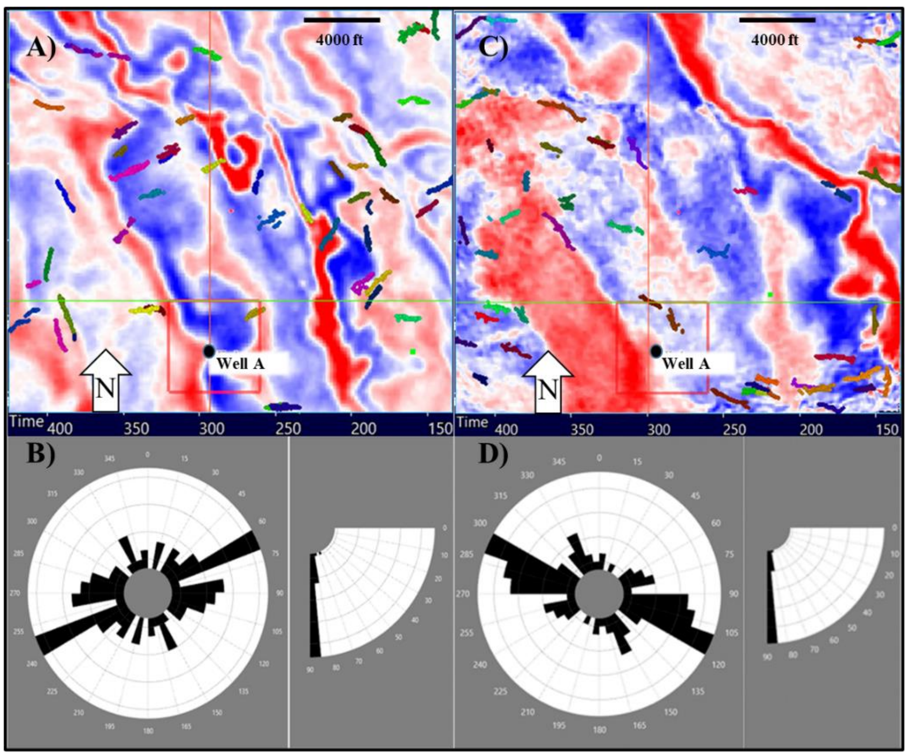

Figure 22 A) time slice at 2000 ms in PP data B) Rose diagram of PP fractures C) time slice at 2000 ms of PS fractures D) Rose diagram of PS fractures.

In order to establish some ground truth to the fractures extracted within the seismic PP and PS data, the fractures generated in the PP and PS volumes were compared to the dipole-dipole shear wave sonic log at the well location. Both PP and PS data showed fractures located near the well which were used to compare to the log. First, the PP volume imaged a fracture nearest the well with a strike orientation of about 60-70 degrees (fig. 23a). The PS data in figure 23b showed a different trend near the well of roughly 150 degrees. Although these are different trends, the actual dominant trend at the well location is 150 degrees with a secondary trend ranging from about 60-75 degrees (fig. 23c). Looking to figure (23) it can be observed that by using a joint PP-PS fracture characterization, a more complete interpretation can be obtained.

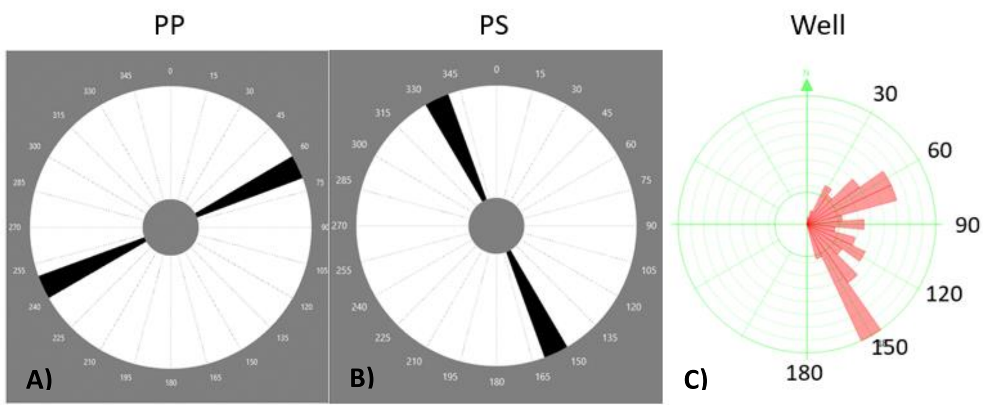

Figure 23 Comparing fractures orientations at the well location as indicated by the PP seismic data (A), the PS seismic data (B) and the dipole-dipole shear wave sonic log (Well A) (C).

CHAPTER V

DISCUSSION AND CONCLUSIONS

5.1 DISCUSSION

Understanding the tectonic stresses acting upon a potential reservoir can prove paramount during the exploration and production phases of a prospect. Identifying fractures, especially in carbonate reservoirs, play a significant role in understanding reservoir quality particularly in unconventional plays. The max horizontal stress in much of central Oklahoma runs dominantly E-W to NE-SW (Snee and Zoback, 2022). To take advantage of this east-west stress trend, the horizontal wells drilled in this area are oriented N-S to run perpendicular to the stress trend to increase fracking efficiency. The use of P-wave seismic data has long been the traditional way of characterizing fractures within a given reservoir. This was done by generating tried and true curvature, coherency, and edge detecting attributes. For an accurate interpretation to be made, it is recommended to use multiple types of data if they are available. Often PS data are collected at the same time as the PP data, so it is suggested to use these available data to help strengthen interpretations.

The large-scale faults identified in both the reprocessed PP and PS data show almost identical trends proving in at least this scale, both datasets have strong similarities. The large-scale faults, trending E-W, show the exact same strike orientation in both PP and PS seismic datasets. The rose diagrams shown in the interpretation section provide evidence that, for the most part, the major fault structure is imaged in both datasets. These similarities give confidence that, moving forward, the differences in fractures imaged can be attributed to the individual properties of the P-wave seismic and PS seismic data.

The fractures extracted in the PS DFN coincided with the various attribute generated. The dominant trend seen in the PS data runs SE to NW with the largest concentration of fractures located in the western most area of the seismic survey. These fractures vary in length from tens of meters to hundreds of meters. The fractures noted in this study lie within the "Mississippian limestones". Fractures located near Well A were compared to the shear wave sonic dipole-dipole log at the same depth, which provided some ground truth to the seismic data and confirmed the results. The majority of these fractures were vertical with only a small quantity dipping between 75-85 degrees.

The fractures imaged from the reprocessed unconditioned PP seismic data, although slightly different, give a unique prospective of how beneficial using joint PP-PS seismic for fracture characterization can be and also how sensitive fracture information truly is. The major strike trend of the fractures imaged in the PP data are shifted slightly and trend mostly from the ENE-WSW. This trend, from fractures imaged nearby the wellbore was also seen at Well A as a secondary dominant strike orientation, further confirming the need for joint PP-PS interpretation. The dip angles from the extracted fractures in the PP data match those seen in the PS data. A high concentration of fractures in the PP data is also observed in the western and easternmost areas of the seismic volume, whereas the PS shows the highest concentration of fractures in the westernmost area only. This is likely the result of the PP data having higher frequencies compared to the PS data at relatively deeper depths.

PP data shows a strong fracture trend at 60 degrees which still shows but less significant in the PS data. The primary strike orientation seen on the PS data ranges from 90 to 120 degrees. This 90-to-120-degree trend is also seen on the PP data; however, it is not as prominent as seen on the PS data. Finally, both PP and PS data show a fracture trend at 150 degrees but is slightly more significant in the PS data (fig. 22). Figure 22a shows a series of fractures located in the southwest corner of the PP data striking in the 150-degree direction, which was observed at multiple parts of the study area by the PP data. the PP and PS data shows fractures in the southwest corner (Figure 22b) with a 150-degree trend.

This difference in fracture distribution and orientation between the PP and PS data can be referred to the fact PP and PS arrivals have different polarization directions, which may affect their ability of resolving steeply dipping features filled with fluids as explained in detail in Stewart et al. (2003). Nevertheless, the difference in fracture distribution and orientation characterized by the PP and PS data in this study is not fully understood. Integrating more wells and well logs in a larger PP-PS seismic survey will definitely assist in constraining and evaluating the PP-PS fracture characterization. An increase in well control within the area is useful in ground truthing fracture orientations. Furthermore, the availability of FMI logs would also drastically increase the confidence of PP-PS fracture interpretations.

5.2 CONCLUSIONS

This study showed that seismic-based characterization work flow can effectively resolve fractures density and orientations in a specific geological formation. The unconditioned PP seismic data seem to show more fractures than the conditioned data, most likely because conditioning may have over smoothed the PP data. Therefore, we recommend careful conditioning or no conditioning of PP data when used for fracture characterization. On the other hand, conditioning the PS data seemed to provide much better results than using unconditioned data. Comparing the interpretation from PP and PS seismic data sets, the following facts were observed:

- Large-scale faults in both PP and PS show strong correlation.
- PS data show more fractures trending in the ESE-WNW direction.

- Reprocessed unconditioned PP data show more fractures trending in the ENE-WSW direction.
- Fractures in both PP and PS can be seen near the wellbore. PP shows 60-degree trend at wellbore, PS shows 150-degree trend at wellbore. Both trends are identified at the well using shear wave dipole-dipole with the strongest being 150 degrees and the secondary being 60 degrees.
- More well control in the area would make for a more confident interpretation.

REFERENCES

Bedell, J. M. A. (2019). *Integrated Fracture and Stress Characterization, Mississippian "Meramec and Osage" Intervals, Stack Play, Central Oklahoma* (Doctoral dissertation, Oklahoma State University).

Blair, K. P., & Berendsen, P. (1988). Subsurface structural geology of the Nemaha tectonic zone. In *Kansas [abstract]: Geological Society of America, South-central Section Meeting Abstracts with Programs* (Vol. 20, No. 2, p. 91).

Berendsen, P., & Blair, K. P. (1995). Structural development of the Nemaha tectonic zone in Kansas. *Circular-Oklahoma Geological Survey*, *97*, 208-214.

Blakey, R. C. (2013). Using paleogeographic maps to portray Phanerozoic geologic and paleotectonic history of western North America. *AAPG Bulletin*, *97*(1), 146.

Cardott, B. J. (1993). *Guidebook for selected stops in the western Arbuckle Mountains, southern Oklahoma* (No. 3). Oklahoma Geological Survey.

Chenin, B., & Joyce, B. (1999). Formation azimuthal anisotropy. *The Leading Edge*, *18*(2), 216-220.

Childress, M., & Grammer, G. M. (2019). Characteristics of debris flows and outrunner blocks—Evidence for Mississippian deposition on a distally steepened ramp.

Chopra, S., & Sharma, R. K. (2019, September). Addressing some artifacts in PP-PS registration prior to performing joint impedance inversion. In *SEG International Exposition and Annual Meeting*. OnePetro.

Comer, J. B., Johnson, K. S., & Cardott, B. J. (1992). Organic geochemistry and paleogeography of Upper Devonian formations in Oklahoma and northwestern Arkansas. In *Source Rocks in the Southern Mid-Continent: 1990 Symposium: Oklahoma Geological Survey Circular* (Vol. 93, pp. 70-93).

Crampin, S. (1985). Evaluation of anisotropy by shear-wave splitting. *Geophysics*, *50*(1), 142-152.

Cubizolle, F., Valding, T., Lacaze, S., & Pauget, F. (2015, October). Global method for seismic-well tie based on real time synthetic model. In *2015 SEG Annual Meeting*. OnePetro.

Davis, Harold G., 1986, Wrenching and oil migration, Mervine field area, Kay County, Oklahoma: Shale Shaker v. 35, p. 1-14; also in Shale Shaker Digest XI, p. 145-158.

da Silva, M. G., Martins, L. O., Junior, J. D., Arruda, M. M., Souza, P., Silva, P. M., ... & Gattass, M. (2014, September). Accelerating Curvature Attributes on GPUs. In *EAGE Workshop on High Performance Computing for Upstream* (pp. cp-426). European Association of Geoscientists & Engineers.

Donati, M., Piazza, J. L., Rollet, A., Baillon, S., Marin, D., Belz, V., Toubiana, H., Castro, J., Bouheouira, A. & Raha, M. (2016). 3D-3C Multicomponent Seismic–A successful fracture characterization case study in Algeria. *first break*, *34*(1).

Droege, L., & Vick, H. (2018). Redefining the STACK play from subsurface to commercialization: Identifying stacked pay sweet spots in the Northern Anadarko Basin. In *AAPG ACE 2018 Annual Convention & Exhibition, Salt Lake City, Utah. Search and Discovery Article* (Vol. 11104).

Gay Jr, S. P. (2003). The Nemaha Trend-A System of Compressional Thrust-Fold, Strike-Slip Structural Features in Kansas and Oklahoma, Part 1.

Gay Jr, S. P. (2003). The Nemaha Trend-A system of compressional thrust-fold, strike-slip structural features in Kansas and Oklahoma,(Part 2, conclusion).

Gupta, M., & Hardage, B. (2017). SV-P: A potential viable alternative to mode-converted P-SV seismic data for reservoir characterization. *Interpretation*, *5*(4), T579-T589.

Kristiansen, P., Gaiser, J. E., & Horne, S. (2005, March). How Multi-Component Seismic Can Be Used To Manage Fractured Carbonate Reservoirs. In *SPE Middle East Oil and Gas Show and Conference*. OnePetro.

McBee, W., Jr., 1999, Discussion: The influence of strike-slip fault systems in the Mid-continent, as illustrated by the Nemaha fault zone: Tulsa Geological Study Group, v. 98-99, no. 5.

Patel, S., Kolawole, F., Walter, J. I., Chen, X., & Marfurt, K. J. (2021). Seismic illumination of small-throw seismogenic faults, Anadarko Basin, Oklahoma. *Interpretation*, *9*(2), SE35-SE51.

Perry, W. J. (1989). *Tectonic evolution of the Anadarko Basin region, Oklahoma* (No. 1866). Department of the Interior, US Geological Survey.

Price, B. J., & Grammer, G. M. (2019). High-resolution sequence stratigraphic architecture and reservoir characterization of the Mississippian Burlington-Keokuk Formation, northwestern Arkansas.

Snee, J. E. L., & Zoback, M. D. (2022). State of stress in areas of active unconventional oil and gas development in North America. *AAPG Bulletin*, *106*(2), 355-385.

Stewart, R. R., Gaiser, J. E., Brown, R. J., & Lawton, D. C. (2002). Converted-wave seismic exploration: Methods. *Geophysics*, *67*(5), 1348-1363.

Stewart, R. R., Gaiser, J. E., Brown, R. J., & Lawton, D. C. (2003). Converted-wave seismic exploration: Applications. *Geophysics*, *68*(1), 40-57.

Stukey, B. C. (2020). *Biostratigraphically constrained ages of Mississippian mixed carbonate-siliciclastic sequences, STACK Play, Anadarko Basin, Oklahoma* (Doctoral dissertation, Oklahoma State University).

Triyoso, W., Oktariena, M., Sinaga, E., & Syaifuddin, F. (2017, April). Full waveform modelling for subsurface characterization with converted-wave seismic reflection. In *IOP Conference Series: Earth and Environmental Science* (Vol. 62, No. 1, p. 012048). IOP Publishing.

Wang, Y., Thompson, T., & Grammer, G. M. (2019). Fracture characterization and prediction in unconventional reservoirs of the "Mississippian Limestone," north-central Oklahoma, United States.

Welker*, C., Feiner, S., Lishansky, R., Phiukhao, W., Chao, J. C., Moore, R., & Hall, D. (2016, August). Trapped Fluid Analysis of 58 Wells from the SCOOP and STACK Plays, Oklahoma. In *Unconventional Resources Technology Conference, San Antonio, Texas, 1-3 August 2016* (pp. 2922-2933). Society of Exploration Geophysicists, American Association of Petroleum Geologists, Society of Petroleum Engineers.

Wittman, B. R. (2013). *Subsurface stratigraphy and characterization of Mississippian (Osagean to Meramecian) carbonate reservoirs of the northern Anadarko Shelf, north-central Oklahoma*. University of Arkansas.

VITA

Michael Dakota Mullen

Candidate for the Degree of

Master of Science

Thesis: COMPARING PP AND PS SEISMIC CHARACTERIZATION OF FRACTURES IN THE MISSISSIPPIAN MERAMEC AND OSAGE INTERVALS OF THE STACK PLAY, OKLAHOMA

Major Field: Geology

Biographical:

Education:

Completed the requirements for the Master of Science in Geology at Oklahoma State University, Stillwater, Oklahoma in May, 2022.

Completed the requirements for the Bachelor of Science in Geology at Oklahoma State University, Stillwater, Oklahoma in 2019.

Experience:

Graduate Teaching Assistant, Boone Pickens School of Geology, Stillwater, Oklahoma, August 2019 to December 2021

Professional Memberships:

American Association of Petroleum Geologists (AAPG)
Society of Exploration Geophysicists (SEG)